THE
PHYSICAL REVIEW

A journal of experimental and theoretical physics established by E. L. Nichols in 1893

SECOND SERIES, VOL. 94, NO. 4 MAY 15, 1954

Magneto-Hydrodynamic Waves in Liquid Sodium

BO LEHNERT
Royal Institute of Technology, Stockholm, Sweden
(Received August 28, 1953)

Liquid sodium, because of its higher electrical conductivity and lower density, is more suitable than mercury for magneto-hydrodynamic experiments. Torsional waves in liquid sodium have been generated in a cylindrical vessel with the axis parallel to a homogeneous magnetic field, and resonance phenomena have been investigated at constant frequency and variable magnetic field strength. The agreement between theory and experiment is satisfactory. It is shown that even with sodium, damping plays an important role under laboratory conditions. The calculations of this paper are also used to improve the results of earlier investigations with mercury.

1. INTRODUCTION

DURING the last ten years the importance of magneto-hydrodynamic phenomena in cosmic physics has been realized in a great number of applications, such as solar physics, cosmic radiation, and the problem of oscillating stars. The investigations of general physical interest made by a number of authors is given in a survey by Lundquist.[1] By far the largest part of the work on magnetohydrodynamics is of a theoretical nature, and there exist only a few experimental investigations, all carried out with mercury.[2–4]

When the theory is applied to special problems in cosmic physics, an exact solution often leads to great mathematical difficulties. Thus, in addition to being a valuable verification of theory, the experimental work serves the purpose of solving problems associated with complicated geometrical configurations through model experiments in the laboratory.[5]

When treating an electrically conducting liquid in a magnetic field from both a theoretical and an experimental point of view, an analogy between magnetic field lines and elastic strings given by Alfvén[5,6] is often a convenient tool. A motion of the liquid perpendicular to the magnetic field gives rise to induced currents and an induced magnetic field. If the conductivity is infinite, the total magnetic field is "frozen in" and the fieldlines act as elastic strings "glued to" the elements of the liquid. This is true in many cosmic applications where the conductivity is high and the dimensions are large. Virtually undamped magneto-hydrodynamic waves are then propagated along the magnetic fieldlines with a velocity independent of frequency in much the same way as elastic waves along strings. However, under laboratory conditions, e.g., in experiments with mercury, the properties of the waves differ from those of "ideal waves," i.e., waves in a liquid with very large conductivity, both at low and high frequencies. The wavelength at low frequencies becomes much larger than the linear dimensions of the apparatus and the wave velocity depends on frequency. At high frequencies the inertia of the liquid becomes too large, and the waves are changed into strongly damped skin waves in a solid body, which also suffer from dispersion. If the conditions are favorable enough, however, there exists an intermediate "ideal" region of frequencies, where the waves are propagated with approximately constant velocity and moderate damping. The condition for such well developed magneto-hydrodynamic wave phenomena is[1,3]

$$BL\sigma\cdot(\mu/\rho)^{\frac{1}{2}}\gg 1, \qquad (1)$$

where B is the magnetic field strength,[7] L the linear di-

[1] S. Lundquist, Arkiv Fysik **5**, 297 (1952).
[2] J. Hartmann and F. Lazarus, Kgl. Danske Videnskab. Selskab, Mat.-fys. Medd. **15**, No. 6 (1937); J. Hartmann, Kgl. Danske Videnskab. Selskab, Mat.-fys. Medd. **15**, No. 7 (1937).
[3] S. Lundquist, Phys. Rev. **76**, 1805–1809 (1949).
[4] B. Lehnert, Arkiv Fysik **5**, No. 5, 69 (1952); Tellus **4**, No. 1, 63 (1952).
[5] H. Alfvén, *Cosmical Electrodynamics* (Oxford University Press, London, 1950).
[6] H. Alfvén, Arkiv mat. astron. fysik **B29**, No. 2 (1942).
[7] Mks units are used throughout this paper. The unit for magnetic field strength is volt sec/m^2 = 10^4 gauss.

TABLE I. Values of the left-hand side of the inequality (1) at different applications. Large values of this quantity correspond to states of motion greatly influenced by electrodynamic forces.

Application	B (volt sec m^{-2})	L (m)	σ (Ω^{-1} m^{-1})	ρ (kg m^{-3})	$BL\sigma\cdot(\mu/\rho)^{\frac{1}{2}}$
Experiments with mercury	1	0.1	10^6	13 600	1
Experiments with liquid sodium	1	0.1	14×10^6	970	50
Sunspots	0.01	10^8	10^6	10^3	3×10^6
Magnetic variable star	1	10^{10}	10^6?	10^3?	3×10^{11}?
Interstellar space	10^{-12}?	10^{22}	10^3?	10^{-21}?	3×10^{19}?

mensions, σ the electric conductivity, ρ the density, and μ the (absolute) permeability. Some possible values of the left-hand side of the expression (1) are given in Table I. It is shown in the table that cosmic conditions are far from being realized in laboratory experiments. Nevertheless the conditions of the experiments with sodium, described in this paper, are improved to such an extent compared to earlier experiments with mercury that it has been worth while to make an experimental investigation with liquid sodium.

The following sections will give an account of some experimental and theoretical investigations of magnetohydrodynamic waves in liquid sodium in the "ideal" region. Section 2 gives a description of the experimental equipment, and a theory of cylindrical waves is presented in Sec. 3. The results are discussed in Sec. 4, and an application to earlier measurements is given in Sec. 5.

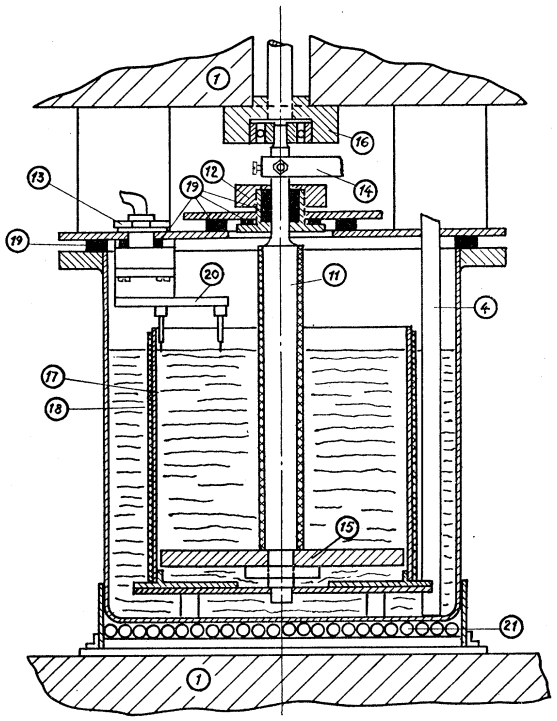

FIG. 1. Outline of the vessel where the waves are generated. 1—Magnet with pole shoes. 4—Pipe for sodium. 11—Axis, isolated with a glass cylinder. 12—Box with packing. 13—Duct bolt. 14—Driving arm. 15—Copper disk. 16—Holder with ball bearing. 17—Cylinder made of brass. 18—Layer of glass tape and silicone resin. 19—Packings of rubber. 20—Probes with holder. 21—Heater.

2. THE EXPERIMENT

(i) The Apparatus

In the experiment, torsional waves are generated in an insulated column of liquid sodium (Fig. 1) placed in a homogeneous, axial magnetic field the strength of which is varied in the range 0.3–1 volt sec/m^2. A copper disk at the bottom of the column is set into oscillations about a vertical axis and generates torsional magnetohydrodynamic waves which are propagated through the liquid along the magnetic field lines to the free surface. There they give rise to an electric potential difference, which is measured by two probes. A frequency of 30 cps has been used.

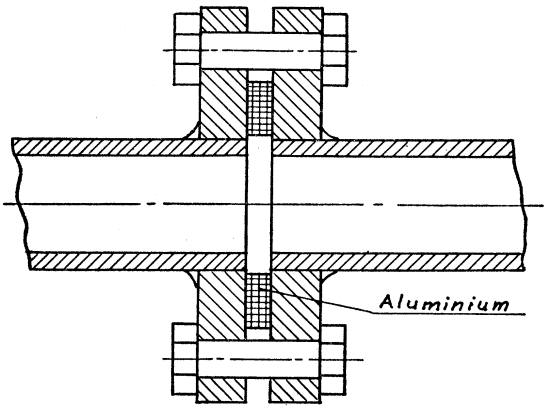

FIG. 2. Joint between two parts of the pipe containing sodium.

To keep the surface of the liquid clean and prevent fire, the interior of the apparatus contains an atmosphere of pure nitrogen. The details are made of nonmagnetic materials, which are not chemically attacked by liquid sodium. Thus the vessels and pipes are made of stainless (nonmagnetic) steel, and the packings in the pipe containing sodium are made of aluminum (Fig. 2). Brass has been chosen with good result for details which are unimportant as regards security and which are not subject to considerable mechanical strain. As shown, e.g., in Fig. 1 all packings not in direct contact with sodium are made of temperature-resistant rubber. A nonconducting surface as that of the inner cylinder in Fig. 1 is obtained by coating a cylinder of brass with glass tape and silicone resin, baked for about 3 hours at 250°C.

Figure 3 is a diagram showing the arrangement of the apparatus. The liquid sodium in the vessel A, which is placed in the magnetic field, is taken from the reservoir B through the pipe C. The levels in the vessels are regulated through the taps J with nitrogen from the

tube *E*. The gas is cleaned in the tube *F* containing pulverized copper at 250°C. The heaters keep the vessels and the middle pipe at about 120°C, controlled by the thermo elements *G*. The parts containing sodium are shielded by sand as shown by the lined regions in Fig. 3. The position of the surface is indicated by signal lamps *H*.

The copper disk at the bottom is set into oscillations through an eccentric shaft, driven by a motor. The vessel in Fig. 1 is strapped between the pole shoes to prevent shaking.

When handling the apparatus, the author wore asbestos clothing as a safety precaution.

(ii) The Method of Measurement

The potential difference at the surface of the liquid is measured by probes placed as shown in Fig. 4. The impedance of the external circuit is very large compared to that of the liquid. Since the diameter of the probes is

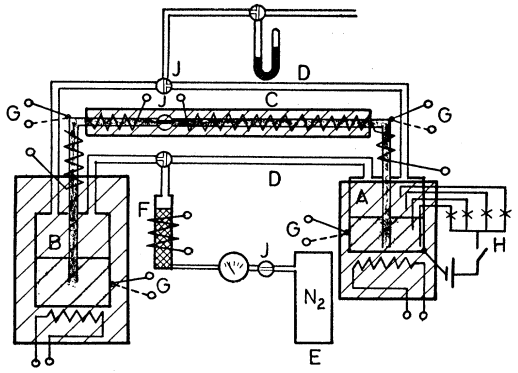

FIG. 3. Sodium system in outline. *A*—Vessel placed in magnetic field. *B*—Reservoir. *C*—Pipe for sodium. *D*—Pipes for nitrogen. *E*—Tube for nitrogen. *F*—Gas-cleaning equipment. *G*—Thermo elements. *H*—Signal lamps. *J*—Taps.

only 0.5 mm, the disturbance caused by the measuring equipment is assumed to be negligible. Above the surface (medium III, which also contains the wires) a homogeneous, axial magnetic field $\mathbf{B}_0$ is assumed since the displacement current can be neglected at low frequencies, and it is shown in Sec. 3 (ii) that the induced currents give no external magnetic field.

The closed paths *ACEDBA*, *ACFDBA*, and *CEDFC* are called C, C_3, and C_1, respectively, where *CFD* has been chosen immediately under the surface and *CED* is an arbitrary path in the liquid. Since the electric field is

$$\mathbf{E}=-\nabla V-\partial\mathbf{A}/\partial t,$$

we have

$$\oint_{C_3}\mathbf{E}\cdot\mathbf{ds}=-\frac{\partial}{\partial t}\oint_{C_3}\mathbf{A}\cdot\mathbf{ds}=-\frac{\partial}{\partial t}\int\int_{C_3}\mathbf{n}\cdot\mathbf{B}_0 dS=0. \quad (2)$$

Further,

$$\mathbf{E}_{\mathrm{III}}=-\nabla V_{\mathrm{III}},$$

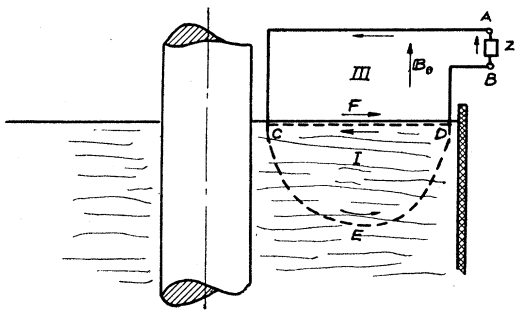

FIG. 4. Calculation of the potential difference between the probes at the surface of a moving liquid in a homogeneous magnetic field $\mathbf{B}_0$. Z is the impedance of the external circuit.

which results in a measured potential difference

$$V_{BA}=\int_{CFD}\mathbf{E}\cdot\mathbf{ds}, \quad (3)$$

if the potential drop in the wires is neglected. The same result is deduced for the arbitrary path C, since

$$\oint_{C_1}\mathbf{E}\cdot\mathbf{ds}=\oint_{C}\mathbf{E}\cdot\mathbf{ds}=\int_{CED}\mathbf{E}\cdot\mathbf{ds}+V_{BA}$$

due to Eq. (2), and Eq. (3) is obtained from the first and last member.

The measurements are carried out with the arrangement shown in Fig. 5. The amplitude of the potential difference V_{BA} is measured with the switch J in "direct" position. The amplified signal is measured with a harmonic wave analyzer *H*. The cathode-ray tube *G* and the wave analyzer *H* are adjusted to the right frequency with the oscillator *F*, whereupon the excited frequency in the vessel *A* is adjusted until the pattern on the tube *G* is stationary.

The phase of the potential difference V_{BA} at the surface is measured with the compensating apparatus shown in the lower left-hand corner of Fig. 5, when the switch J is in the upper position. The eccentric shaft *B* affects the strain gauge *C* giving rise to a compensating voltage over the resistance R_2. The phase of the voltage

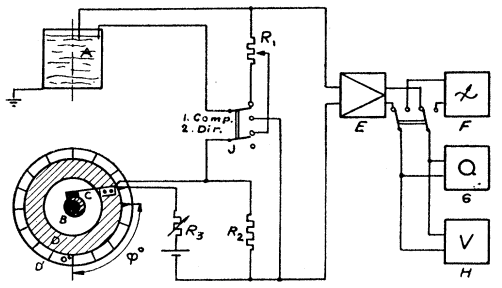

FIG. 5. Diagram of the method of measurement: *A*—Vessel with probes. *B*—Axis with eccentric shaft. *C*—Strain gauge. *D*—Holder. *D'*—Scale. *E*—Amplifier. *F*—Signal generator. *G*—Cathode-ray oscillograph. *H*—Harmonic wave analyzer.

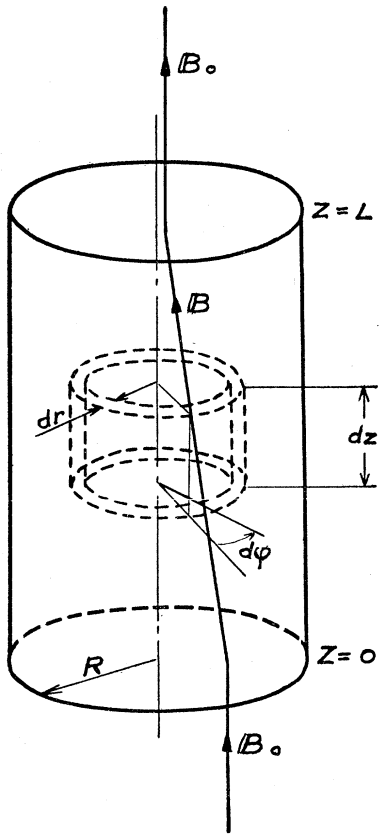

FIG. 6. Twisting of a cylindrical column of liquid with infinite conductivity placed in an axial homogeneous magnetic field $\mathbf{B}_0$.

at the surface is given by the scale D' when the holder D and resistance R_3 are adjusted to give the resulting voltage zero at H. The zero point of the scale D' is determined at maximum magnetic field (1 volt sec/m^2) and lowest possible frequency (about 5 cps).

3. THEORY OF THE EXPERIMENT

(i) Cylindrical Waves at Infinite Conductivity

Before an exact treatment is carried out let us consider a simple example in a liquid with density ρ and infinite electrical conductivity. If a magnetic field $\mathbf{B}_0$ is assumed to exist within the liquid, no relative motion between the magnetic lines of force and the liquid is possible, since such a motion would give rise to infinitely large currents (see, e.g., reference 5). Consider a column of height L and radius R (Fig. 6), which is parallel to the field and has been twisted with constant pitch φ_0/L. Cylindrical coordinates are introduced, and the field is written

$$\mathbf{B}=(0,b,B_0),$$

where $b=B_0\cdot r\cdot\varphi_0/L$ is the component due to the twisting. The increase of magnetic energy is

$$U=\int_0^R (b^2/2\mu)\cdot L2\pi r dr=(B_0^2/2\mu)\cdot\tfrac{1}{2}\pi R^2\cdot\varphi_0^2/L. \quad (4)$$

From the theory of elasticity it is known that the corresponding expression for the torque of an elastic rod with a modulus G of torsional rigidity is

$$M=G\cdot\tfrac{1}{2}\pi R^4\cdot\varphi_0/L \quad (5)$$

and the potential energy

$$U=\int_0^{\varphi_0} M\cdot d\varphi=G\cdot\tfrac{1}{2}\pi R^4\cdot\tfrac{1}{2}\varphi_0^2/L. \quad (6)$$

From the results (4) and (6) we define an equivalent modulus

$$G_{\text{eq}}=B_0^2/\mu. \quad (7)$$

The dynamic equation of a disk with height dz is given by (5):

$$G_{\text{eq}}\cdot\tfrac{1}{2}\pi R^4\cdot\frac{\partial^2\varphi}{\partial z^2}=\frac{\partial}{\partial t}\left[\int_0^R r^2\cdot\frac{\partial\varphi}{\partial t}\rho\cdot 2\pi r\cdot dr\right],$$

which becomes

$$\frac{\partial^2\varphi}{\partial t^2}=\left(\frac{G_{\text{eq}}}{\rho}\right)\cdot\frac{\partial^2\varphi}{\partial z^2}, \quad (8)$$

where the wave velocity is

$$V=(G_{\text{eq}}/\rho)^{\frac{1}{2}}=B_0/(\mu\rho)^{\frac{1}{2}}. \quad (9)$$

If all quantities are assumed to vary harmonically in time the solutions of (8) have the form

$$\varphi=[Ae^{i\omega z/V}+Be^{-i\omega z/V}]e^{i\omega t}.$$

If the boundary conditions,

$$\varphi(0,t)=\varphi_0 e^{i\omega t} \quad \text{at} \quad z=0$$

and

$$M(L,t)=0 \quad \text{at} \quad z=L,$$

are imposed we get the motion at the free surface $z=L$ of a column of liquid which is in a state of torsional oscillations with a given amplitude at the bottom, $z=0$:

$$\varphi(L,t)=\varphi_0 e^{i\omega t}/\cos(\omega L/V). \quad (10)$$

(ii) Cylindrical Waves with Negligible Viscous Damping

The notations shown in Fig. 7 are used in the calculations of the waves generated in the apparatus described in Sec. 2. The column of sodium (region I), which has the electrical conductivity σ_1 and density ρ, is bounded at the nonconducting surfaces $r=r_0$ and $r=R$. The copper disk at the bottom (region II) has the conductivity σ_2 and thickness δ. Since the viscosity can be omitted[3] the following boundary conditions are imposed:

(1) The radial component i_r of current density vanishes at $r=R$ in regions I and II and at $r=r_0$ in region I.

(2) The axial component, i_z, vanishes at the surface $z=L$.

(3) The result of the following analysis shows that the influence of the sodium layer between the disk and the bottom is equivalent to a slight increase in the thickness δ. Thus the boundary condition at the bottom is approximated to

$$i_z(r, -\delta, t)=0.$$

(4) The solutions in regions I and II are fitted at the boundary $z=0$, where the axial component i_z and the tangential components h_φ and E_z are continuous. h_φ is the induced magnetomotive force ($\mathbf{b}=\mu\mathbf{h}$).

(5) The mechanical influence of the axis is estimated with the results of Sec. 2. At a magnetic field strength $B_0=1$ Vs/m^2 the equivalent modulus of rigidity is

$$G_{Na}=B_0^2/\mu=7.80\times10^5 \text{ newtons/m}^2,$$

whereas an axis made of steel has a modulus of about

$$G_a=7.85\times10^{10} \text{ newtons/m}^2.$$

In this case we have $R=0.068$ m and the radius of the axis $r_a=0.010$ m. At a given twisting, $\partial\varphi/\partial z$, the ratio of the corresponding torques is given by (5):

$$M_{Na}/M_a=(R/r_a)^4\cdot G_{Na}/G_a=0.02.$$

Thus, with the dimensions given in Fig. 7, the mechanical influence of the axis can be neglected, and the velocity of the copper disk is

$$v^{(II)}=v_0\cdot(r/R)\cdot e^{j\omega t}=\Omega_0 r e^{j\omega t}, \tag{11}$$

where Ω_0 is the peak value of the angular velocity of the axis and ω the frequency.

A general treatment of magneto-hydrodynamic waves has been given in earlier works[1,8] and will not be described in detail here. If the liquid and the disk in Fig. 7 are assumed to oscillate around the axis of symmetry and a homogeneous magnetic field $\mathbf{B}_0=\mu\mathbf{H}_0$, parallel with the axis, is generated by external sources, then an induced emf. will arise in a direction perpendicular to the axis. Thus the induced currents will flow in planes through the axis and the induced magnetic field is parallel with the particle velocity. It is shown in the following that the induced magnetic field disappears at the free surface and the bottom of the vessel (see Fig. 7), and the total magnetic field becomes homogeneous all over the region outside the vessel [see Sec. 2 (ii)]. The general solution of a cylindrically symmetric state of torsional oscillations with frequency ω is discussed in the system of cylindrical coordinates given by Fig. 7:

$$\begin{aligned}&\partial/\partial\varphi=0, \quad \partial/\partial t=j\omega,\\ &\mathbf{v}=(0,v,0), \quad \mathbf{h}=(0,h,0), \quad \mathbf{H}_0=(0,0,H_0),\\ &\mathbf{i}=(i_r,0,i_z), \quad \mathbf{E}=(E_r,0,E_z), \quad \mathbf{H}=\mathbf{H}_0+\mathbf{h},\end{aligned} \tag{12}$$

where $\mathbf{v}$ is the velocity of the liquid and $\mathbf{b}=\mu\mathbf{h}$ the induced magnetic field. At low frequencies the displacement current can be neglected, and the fundamental

[8] C. Walén, Arkiv mat. astron. fysik **A30**, No. 15 (1944).

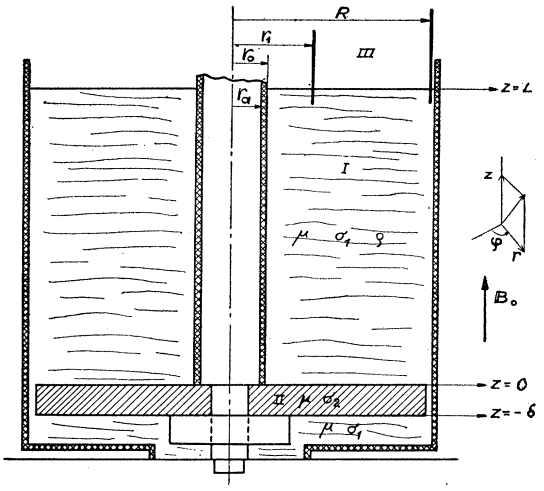

FIG. 7. Notation and starting points for the calculation described in Sec. 3. Inner radius of the outer, nonconducting cylinder and position of outer probe, $R=6.8$ cm. Outer radius of glass cylinder at the axis, $r_0=1.2$ cm. Position of inner probe, $r_1=3.2$ cm. Radius of axis, made of stainless steel, $r_a=1$ cm. Height of the column of liquid sodium, $L=10.5$ cm. Thickness of the copper disk at the bottom, $\delta=1$ cm.

equations at constant permeability μ are

$$\begin{aligned}&\text{curl}\mathbf{h}=\mathbf{i},\\ &\text{curl}\mathbf{E}=-\mu\partial\mathbf{h}/\partial t,\\ &\text{div}\mathbf{h}=0,\\ &\mathbf{i}=\sigma[\mathbf{E}+\mu\cdot(\mathbf{v}\times\mathbf{H})].\end{aligned} \tag{13}$$

In the liquid, which is incompressible, are added the conditions

$$\begin{aligned}&\rho\frac{d\mathbf{v}}{dt}=\mu\cdot(\mathbf{i}\times\mathbf{H})-\text{grad}p,\\ &\text{div}\mathbf{v}=0,\end{aligned} \tag{14}$$

where p is the hydrostatic pressure. In the copper disk the condition expressed in Eq. (11) is added to the system (13). The solution at small amplitudes is:

Solution in Region I

The equations for cylindrical waves are deduced from the expressions (13) and (14):[3]

$$\begin{aligned}&\frac{\partial^2 h}{\partial t^2}=\frac{1}{\mu\sigma_1}\cdot\frac{\partial}{\partial t}\left[\frac{\partial^2 h}{\partial r^2}+\frac{1}{r}\frac{\partial h}{\partial r}-\frac{h}{r^2}+\frac{\partial^2 h}{\partial z^2}\right]+V^2\frac{\partial^2 h}{\partial z^2},\\ &\frac{\partial v}{\partial t}=(\mu H_0/\rho)\cdot\frac{\partial h}{\partial z}, \quad V^2=(\mu/\rho)\cdot H_0^2.\end{aligned} \tag{15}$$

The first equation has the form

$$\frac{\partial^2 h}{\partial r^2}+\frac{1}{r}\frac{\partial h}{\partial r}+\left(k^2-\frac{1}{r^2}\right)h=0, \tag{16}$$

with

$$\gamma^2=(k^2+j\omega\mu\sigma_1)/(1+\mu\sigma_1V^2/j\omega), \tag{17}$$

for travelling waves, where all quantities vary as $\exp(j\omega t+\gamma z)$. The solutions of (16) have the form

$$h^{(\mathrm{I})}=[A'J_1(kr)+B'N_1(kr)][C'e^{\gamma z}+e^{-\gamma z}]e^{j\omega t}. \tag{18}$$

The constants A' and B' are determined by the boundary conditions

$$i_r(r_0,z,t)=i_r(R,z,t)=0,$$

which give

$$\begin{aligned} A'J_1(kr_0)+B'N_1(kr_0)&=0,\\ A'J_1(kR)+B'N_1(kR)&=0, \end{aligned} \tag{19}$$

since $i_r=-\partial h/\partial z$. The solution of (19) corresponds to a number of modes with possible values k_ν determined by

$$J_1(k_\nu r_0)N_1(k_\nu R)-J_1(k_\nu R)N_1(k_\nu r_0)=0. \tag{20}$$

The condition at the surface,

$$i_z(r,L,t)=0,$$

gives the relation

$$C'e^{\gamma L}+e^{-\gamma L}=0, \tag{21}$$

since

$$i_z=\frac{1}{r}\frac{\partial}{\partial r}(rh).$$

If we introduce

$$Z_1(k_\nu r)=J_1(k_\nu r)-\frac{J_1(k_\nu r_0)}{N_1(k_\nu r_0)}N_1(k_\nu r) \tag{22}$$

and B' is eliminated by means of Eq. (19), a particular solution of (16) becomes

$$h^{(\mathrm{I})}=A'Z_1(k_\nu r)e^{-\gamma L}[e^{\gamma(L-z)}-e^{-\gamma(L-z)}]e^{j\omega t}. \tag{23}$$

Finally, from the expressions (13) and (15),

$$E_r=i_r/\sigma_1-\mu H_0 v, \quad v=(\mu H_0/j\omega\rho)(\partial h/\partial z). \tag{24}$$

Thus the general solution in region I has the form

$$\begin{aligned} h^{(\mathrm{I})}&=\sum_{\nu=1}^{\infty}A_\nu^{(\mathrm{I})}Z_1(k_\nu r)\sinh[\gamma_\nu(L-z)]e^{j\omega t},\\ i_z^{(\mathrm{I})}&=\sum_{\nu=1}^{\infty}k_\nu A_\nu^{(\mathrm{I})}Z_0(k_\nu r)\sinh[\gamma_\nu(L-z)]e^{j\omega t},\\ E_r^{(\mathrm{I})}&=\sum_{\nu=1}^{\infty}(\gamma_\nu/\sigma_1)(1+\mu\sigma_1V^2/j\omega)A_\nu^{(\mathrm{I})}Z_1(k_\nu r)\\ &\qquad\times\cosh[\gamma_\nu(L-z)]e^{j\omega t},\\ v^{(\mathrm{I})}&=\sum_{\nu=1}^{\infty}-(\mu H_0\gamma_\nu/j\omega\rho)A_\nu^{(\mathrm{I})}Z_1(k_\nu r)\\ &\qquad\times\cosh[\gamma_\nu(L-z)]e^{j\omega t}. \end{aligned} \tag{25}$$

Solution in Region II

From the fundamental equations (13) and the condition (11), the equations for region II are deduced

$$\begin{aligned} -\partial h/\partial z&=\sigma_2E_r+\mu\sigma_2H_0v,\\ -\partial^2h/\partial z^2&=\sigma_2\partial E_r/\partial z, \end{aligned}$$

and

$$\frac{1}{r}\frac{\partial}{\partial r}(rh)=\sigma_2E_z,$$

which is combined with

$$\frac{\partial E_r}{\partial z}=\frac{\partial E_z}{\partial r}-j\omega\mu h,$$

giving

$$\frac{\partial^2h}{\partial r^2}+\frac{1}{r}\frac{\partial h}{\partial r}-\frac{h}{r^2}+\frac{\partial^2h}{\partial z^2}-\mu\sigma_2\frac{\partial h}{\partial t}=0. \tag{26}$$

Equation (26) is also obtained by putting $\rho=\infty$, $V=0$ in the first expression (15).

A separation in the usual manner leads to the particular solution

$$h^{(\mathrm{II})}=[A''J_1(kr)+B''N_1(kr)][C''e^{\kappa z}+e^{-\kappa z}]e^{j\omega t}, \tag{27}$$

where

$$\kappa^2=k^2+j\omega\mu\sigma_2. \tag{28}$$

A small error is committed in neglecting the currents in the region $r<r_0$ at the junction of the disk and the axis. With this approximation the radial boundary conditions become the same as in region I, and the modes are given by (20). With

$$i_z(r,-\delta,t)=0,$$

an analogous treatment gives the general solution in region II:

$$\begin{aligned} h^{(\mathrm{II})}&=\sum_{\nu=1}^{\infty}A_\nu^{(\mathrm{II})}Z_1(k_\nu r)\sinh[\kappa_\nu(z+\delta)]e^{j\omega t},\\ i_z^{(\mathrm{II})}&=\sum_{\nu=1}^{\infty}k_\nu A_\nu^{(\mathrm{II})}Z_0(k_\nu r)\sinh[\kappa_\nu(z+\delta)]e^{j\omega t},\\ E_r^{(\mathrm{II})}&=\sum_{\nu=1}^{\infty}-(\kappa_\nu/\sigma_2)A_\nu^{(\mathrm{II})}Z_1(k_\nu r)\cosh[\kappa_\nu(z+\delta)]e^{j\omega t}\\ &\qquad-\mu H_0\Omega_0re^{j\omega t},\\ v^{(\mathrm{II})}&=\Omega_0re^{j\omega t}. \end{aligned} \tag{29}$$

The velocity distribution v_{II} is now developed into modes

$$\Omega_0r=\sum_{\nu=1}^{\infty}W_\nu Z_1(k_\nu r); \quad r_0\leqslant r\leqslant R. \tag{30}$$

From the orthogonality relations the coefficients W_ν are

derived in the usual manner:[9]

$$W_\nu = -2\cdot\frac{\Omega_0 R}{k_\nu R Z_0(k_\nu R)} \times\frac{1-(r_0/R)^2[Z_0(k_\nu r_0)/Z_0(k_\nu R)]}{1-(r_0/R)^2[Z_0(k_\nu r_0)/Z_0(k_\nu R)]^2}. \quad (31)$$

Fitting of the Solutions at the Boundary $Z=0$

The field quantities i_z, E_r, and h of the νth partial wave given by (25) and (29) are fitted at the boundary $z=0$:

$$A_\nu^{(\mathrm{I})}\sinh(\gamma_\nu L)=A_\nu^{(\mathrm{II})}\sinh(\kappa_\nu\delta),$$
$$(\gamma_\nu/\sigma_1)(1+\mu\sigma_1V^2/j\omega)A_\nu^{(\mathrm{I})}\cosh(\gamma_\nu L) = -(\kappa_\nu/\sigma_2)A_\nu^{(\mathrm{II})}\cosh(\kappa_\nu\delta)-\mu H_0 W_\nu. \quad (32)$$

If

$$\lambda_\nu^2=k_\nu^2+j\omega\mu\sigma_1 \quad (33)$$

is introduced and Eq. (32) is solved for $A_\nu^{(\mathrm{I})}$, the velocity in the liquid is given by (25):

$$v^{(\mathrm{I})}=\sum_{\nu=1}^{\infty} W_\nu Z_1(k_\nu r)\frac{\cosh[\gamma_\nu(L-z)]}{\cosh(\gamma_\nu L)}F_\nu e^{j\omega t}, \quad (34)$$

where

$$\frac{1}{F_\nu}=\left(1+\frac{j\omega}{\mu\sigma_1V^2}\right)\left(1+\frac{\sigma_1}{\sigma_2}\frac{\gamma_\nu\kappa_\nu}{\lambda_\nu^2}\frac{\tanh(\gamma_\nu L)}{\tanh(\kappa_\nu\delta)}\right). \quad (35)$$

The result is illustrated by some special cases.

1. If the conductivities σ_1 and σ_2 tend to infinity, we have

$$\gamma_\nu=j\omega/V \quad \text{and} \quad F_\nu=1.$$

Thus

$$v^{(\mathrm{I})}=\Omega_0 r\frac{\cos[(L-z)/V]}{\cos[\omega L/V]}e^{j\omega t},$$

which is the expression for an ideal column of liquid discussed in Sec. 2 (see also the discussion of convergence at the end of this paragraph).

2. With finite conductivities and vanishing thickness of the disk, $v^{(\mathrm{I})}$ tends to zero.

3. If the magnetic field B_0 tends to infinity, we have

$$v^{(\mathrm{I})}=\Omega_0 r e^{j\omega t},$$

and the liquid behaves like a solid attached to the disk at the bottom.

4. If the disk at the bottom is assumed to be ideal ($\sigma_2=\infty$), the factors F_ν tend to the value

$$F_\nu=1/(1+j\omega/\mu\sigma_1V^2).$$

In particular, if $r_0=0$ and $\omega/\mu\sigma_1V^2\ll 1$, the formula given by Lundquist[3] is obtained:

$$v^{(\mathrm{I})}=\Omega_0 R\sum_{\nu=1}^{\infty}\frac{2J_1(k_\nu r)}{k_\nu r J_2(k_\nu R)}\frac{\cosh[\gamma_\nu(L-z)]}{\cosh(\gamma_\nu L)}e^{j\omega t}. \quad (36)$$

Indicated Potential Difference at the Surface

The potential difference between the probes at the points $r=r_1$ and $r=R$ is

$$V_{r_1R}=\int_{r_1}^{R}E_r^{(\mathrm{I})}dr,$$

as shown in Sec. 2 (ii), Eq. (3). Since

$$E_r^{(\mathrm{I})}=-(1+j\omega/\mu\sigma_1V^2)B_0v^{(\mathrm{I})}$$

and

$$\int_{r_1}^{R}Z_1(k_\nu r)dr=-(1/k_\nu)[Z_0(k_\nu r)]^R{}_{r_1},$$

the voltage at the surface is found by integrating (34):

$$V_{r_1R}=(1+j\omega/\mu\sigma_1V^2)B_0\sum_{\nu=1}^{\infty}(W_\nu/k_\nu) \times[Z_0(k_\nu R)-Z_0(k_\nu r_1)]F_\nu e^{j\omega t}/\cosh(\gamma_\nu L). \quad (37)$$

The asymptotic value for $B_0\to\infty$ is

$$V_{r_1R}(B_0\to\infty)\to-\Omega_0B_0\tfrac{1}{2}(R^2-r_1^2),$$

from which a normalized voltage $U=V_{r_1R}/V_{r_1R}(B_0\to\infty)$ is defined:

$$U=\underbrace{(1+j\omega/\mu\sigma_1V^2)}_{(a)}\cdot\underbrace{\frac{4}{1-(r_1/R)^2}}_{(b)}\cdot\sum_{\nu=1}^{\infty}\underbrace{\frac{1-Z_0(k_\nu r_1)/Z_0(k_\nu R)}{(k_\nu R)^2}}_{(c)}\cdot\underbrace{\frac{1-(r_0/R)^2[Z_0(k_\nu r_0)/Z_0(k_\nu R)]}{1-(r_0/R)^2[Z_0(k_\nu r_0)/Z_0(k_\nu R)]^2}}_{(d)}\cdot\underbrace{F_\nu e^{j\omega t}/\cosh(\gamma_\nu L)}_{(e)}, \quad (38)$$

where F_ν are given by (35) and the expression (31) for W_ν has been used. The factor (a) is due to the finite conductivity of the liquid forming a part of the measuring circuit, (b) and (c) are due to the position of the inner probe and the special radial velocity distribution which has been chosen, and (d) corresponds to the finite radius of the axis; (e) is the "axial" factor, where F_ν represents the efficiency of the generating mechanism and $1/\cosh(\gamma_\nu L)$ is the factor of main interest which can give rise to resonance phenomena. This factor reduces to $1/\cos(\omega L/V)$ in an ideal liquid.

Discussion of the Convergence

With the asymptotic formulas for $J_p(k_\nu r)$, $N_p(k_\nu r)$ and the roots k_ν (see the tables by Jahnke-Emde[9]), it is easily shown that the remainders, v_n and U_n,

[9] E. Jahnke and F. Emde, *Tables of Functions* (Dover Publications, New York, 1945).

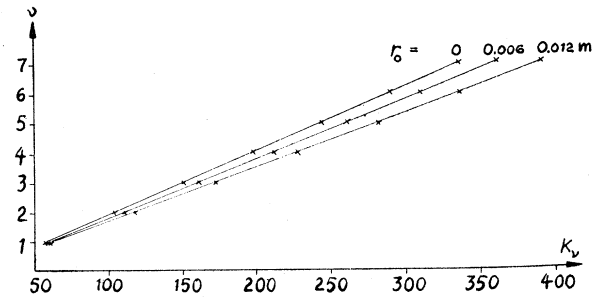

FIG. 8. Values of k_ν as given by (20) for three values of outer radius r_0 of the axis. $r_0=0$ corresponds to the equations $J_1(k_\nu R)=0$.

after n terms of the series (34) and (38) tend to the limits

$$v_n \rightarrow \text{const} \sum_{\nu=n}^{\infty} (1/\nu) \sin(\nu\theta) \times[(r_0/R)^{\frac{1}{2}}+(-1)^\nu]F_\nu \exp[-(a+jb)\nu z/L],$$

$$U_n \rightarrow \text{const}(1+j\omega/\mu\sigma_1 V^2) \sum_{\nu=n}^{\infty} (1/\nu)^2 \cos(\nu\theta_1) \times[(r_0/R)^{\frac{1}{2}}+(-1)^\nu]F_\nu \exp[-(a+jb)\nu],$$

where $a(\geqslant 0)$ and b are functions of σ_1, V, ω and $\lim a=\lim b=0$ when $\sigma_1\rightarrow\infty$ and $\theta=\pi(r-r_0)/(R-r_0)$, $\theta_1=\pi(r_1-r_0)/(R-r_0)$. The remainders are uniformly convergent, even in the limiting case $\sigma_1=\infty$ (see, e.g., Titchmarsh[10] and Hardy[11]).

4. RESULTS OF THE CALCULATIONS AND MEASUREMENTS IN LIQUID SODIUM

The linear dimensions of the apparatus are given in Fig. 7. A magnetic field strength in the range $B_0=0.3-1.0$ volt sec/m^2 and a frequency $\omega=188.5$ sec^{-1} (30 cps) corresponds to a region containing the first resonance of the ideal column of liquid. The temperature is kept at 120°C, corresponding to $\sigma_1=94.0\times10^6$ Ω^{-1} m^{-1} for liquid sodium and $\sigma_2=40.6\times10^6$ Ω^{-1} m^{-1} for copper, and the density of sodium is $\rho=970$ kg/m^3. The axis has been oscillating with a peak angular velocity $\Omega_0=3.84$ sec^{-1}, corresponding to a voltage of the order 10^{-2} volt between the axis and periphery at the bottom when $B_0=1$ volt sec/m^2.

The values k_ν from (20) are shown in Fig. 8. It is seen that they are only slightly modified in the range of values r_0 of the axis given by the figure.

Figures 9(a) and 9(b) show the depth of penetration $1/\alpha_\nu$ and phase velocity ω/β_ν for the five first modes, when the magnetic field is varied. $\gamma_\nu=\alpha_\nu+j\beta_\nu$ is given by (17).

The "axial" factors,

$$S_\nu=F_\nu/\cosh(\gamma_\nu L) \qquad (39)$$

[see Eq. (38)], are shown in Figs. 10(a) and 10(b), where the dotted lines mark the result when the influence of finite conductivity and thickness of the copper disk is neglected ($F_\nu=1$).[12] Thus the influence of the disk is rather small in the actual case. Further, the damping of the waves prevents a formation of resonance maxima of higher order at increasing values of $1/B_0$. The phase difference between bottom and surface [Fig. 10(b)] increases nearly linearly even for the first mode, contrary to the jump of 180° at the resonance when the conductivity is infinite.

The resulting normalized voltage at the surface according to (38) is shown in Figs. 11(a) and 11(b) as well as the corresponding experimental results. The modification of the curves for the first mode ($\nu=1$) depends mainly on the influence of the second mode. The series converges rapidly and the fifth and higher modes become negligible. Thus the sharp resonance of the column with infinite conductivity is reduced by losses in the liquid and the copper disk and through "dispersion" of the composing modes to a barely detectable maximum, displaced in the direction of stronger values of the magnetic field.

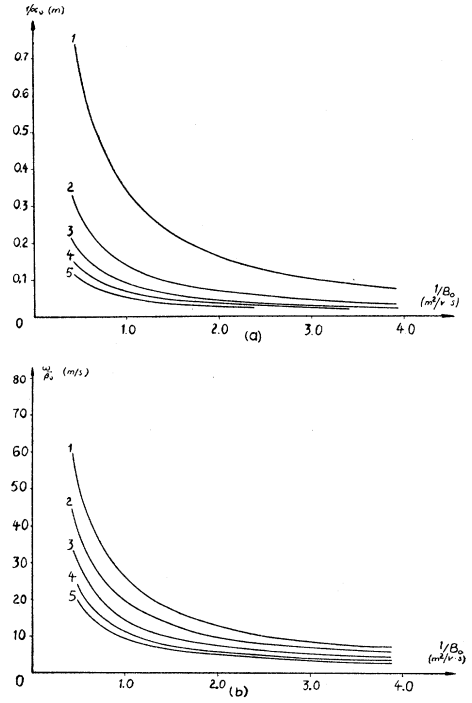

FIG. 9. (a) Depth of penetration, $1/\alpha_\nu$, of cylindrical waves in a column of liquid sodium at 120°C with the dimensions $r_0=0$, $R=6.8$ cm at a frequency $\omega=188.5$ sec^{-1} (30 cps). The five first modes are given. In the experiment $r_0=1.2$ cm and the corresponding curves of Figs. 9 (a), (b) and 10 (a), (b) are modified with less than 10 percent even for the fifth mode. (b) Phase velocity ω/β_ν of the waves.

[10] E. C. Titchmarsh, *The Theory of Functions* (Oxford University Press, London, 1939), p. 42.
[11] G. H. Hardy, *A Course of Pure Mathematics* (Cambridge University Press, Cambridge, 1952), p. 473.

[12] The calculations have been performed with the help of tables and a chart atlas by A. E. Kennelly, *Tables of Complex Hyperbolic and Circular Functions* and *Chart Atlas of Complex Hyperbolic and Circular Functions* (Harvard University Press, Cambridge, 1914).

Even if the phase is measured more precisely than the amplitude, the discrepancy between theory and experiment as regards the amplitude is hardly within the limits of error. The deviation has the same direction as in earlier investigations being greater in the measurement of amplitude than in that of the phase [see Figs. 11 (a), (b) and 12 (a), (b)]. The elasticity of the upper part of the axis in Fig. 1 may introduce an error. Other possible sources of error are mechanical disturbances by the inner probe ($r=r_1$) and impurities of the liquid, the disk at the bottom and the boundary layer between disk and liquid; all these effects increase the apparent damping. An impurity of the free surface may have some mechanical influence but it is not so important as in mercury (Sec. 5). In Sec. 3 it has been pointed out that the currents at the junction of axis and disk and in the layer of sodium below the axis have been neglected. This reduces the effectiveness of the generating mechanism and appears as an increase in the damping when the amplitude at the bottom is kept constant. Finally, the velocity distribution at the bottom has been assumed to have a finite value at $r=R$, which is an approximation when the viscosity is taken into account.

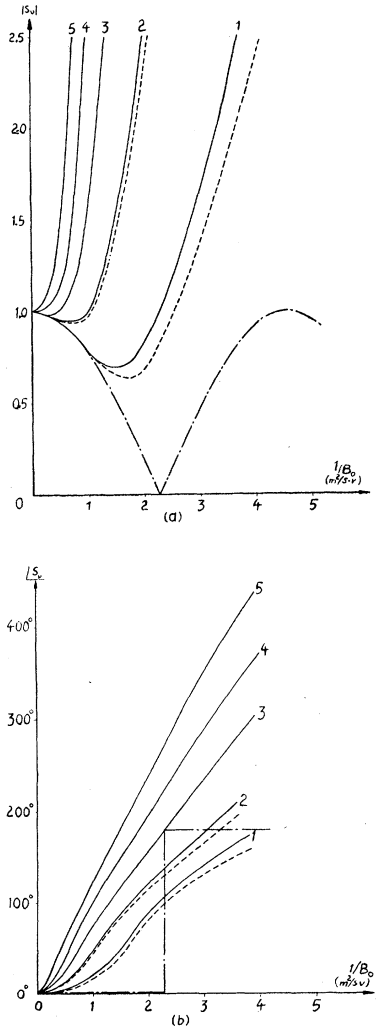

FIG. 10. (a) Amplitude $|S_\nu|$ of the "axial factors" (35), (39) of a column with $r_0=0$, $R=6.8$ cm, $\omega=188.5$ sec^{-1}. —·— column with infinite conductivity; – – – – result when the influence of the disk at the bottom is neglected ($F_\nu=1$); —— resulting theoretical curve; (b) Phase $\angle S_\nu$ of the "axial factors."

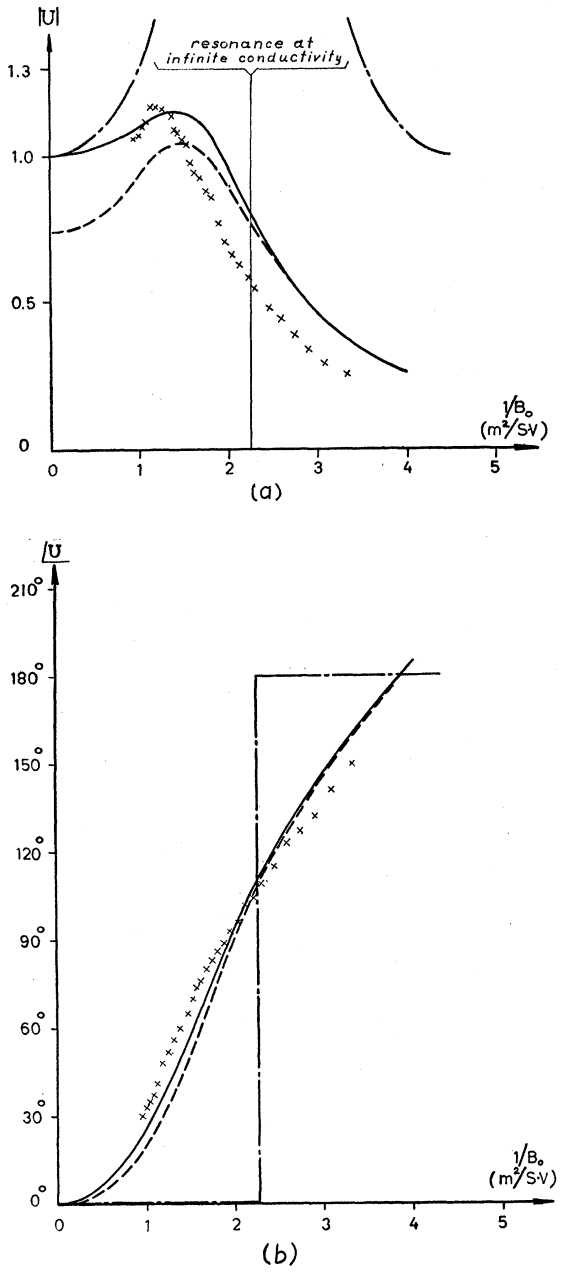

FIG. 11. (a) Amplitude $|U|$ of normalized indicated potential difference at the surface as given by Eq. (38). Linear dimensions according to Fig. 7 and frequency $\omega=188.5$ sec^{-1}. —·— column with infinite conductivity; – – – – first mode ($\nu=1$); —— resulting theoretical curve; ××× measurements. (b) Phase $\angle U$ of the normalized potential difference.

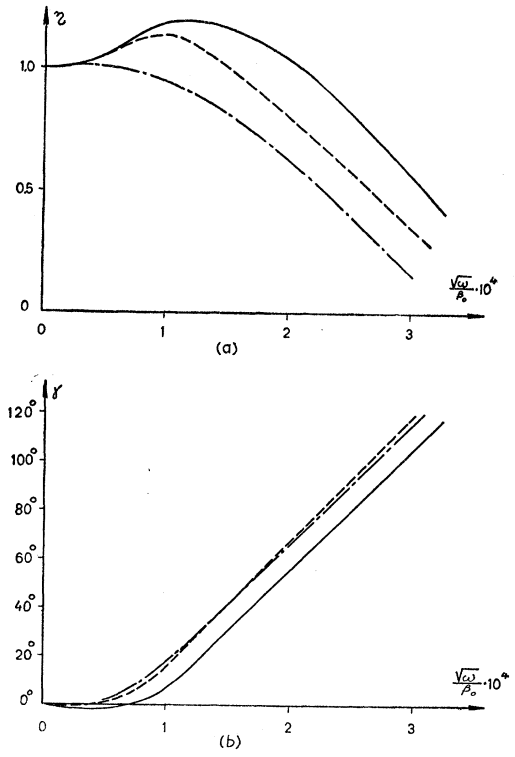

FIG. 12. (a) Amplitude, η, at normalized velocity at the point $r=4.1$ cm at the surface of a vessel with mercury with radius $R=15$ cm and height $L=15$ cm as given by Lundquist.[3] —— theoretical results by Lundquist; —·— experimental results by Lundquist; - - - - theoretical results after application of the factors F_ν given by (35). (b) Phase γ of normalized velocity.

5. A NOTE ON LUNDQUIST'S INVESTIGATIONS

Earlier investigations of cylindrical magneto-hydrodynamic waves have been carried out in mercury[3] with an apparatus similar to that of Fig. 1. The waves were excited with a disk furnished with 1-cm high radial strips and the motion indicated at the surface with a floating mirror and a scale. If the liquid between the strips is treated as a solid disk of mercury, the result (34) may be applied to the velocity $v^{(I)}$. $Z_1(k_\nu r)$ is replaced by $J_1(k_\nu r)$ in this case, where $r_0=0$. The result when the influence of the disk has been included is shown in Figs. 12 (a), (b), which also show the results given by earlier investigations.[13]

[13] Dr. Lundquist has kindly placed his numerical calculations at the author's disposal for the application of the factors F_ν given by (35).

After the application of Eq. (34), however, there still remains a discrepancy for the amplitude [Fig. 12(a)]. It has been pointed out by Lundquist that a source of error may be the tenacious surface layer of mercury. Another possible source is a slipping of the liquid round the strips at the bottom, i.e., the mercury between the strips cannot be considered as a solid. Finally, the inertia of the mirror and impurities of the mercury may introduce some error.

6. CONCLUSION

The investigations of magneto-hydrodynamic waves in sodium and mercury show a satisfactory agreement between theory and experiment. The conditions for model experiments in the laboratory scale, however, cannot give a very good picture of cosmic phenomena, even with such a medium as liquid sodium. A velocity profile with sharp edges, which is demanded, e.g., in an experiment on whirl rings, representing a mechanism for sunspots, becomes rather diffuse and damped after travelling through an experimental arrangement of laboratory dimensions [see Eq. (17) and Figs. 9(a) and 9(b)]. In experiments on resonance phenomena the conditions are more unfavorable since the reflected waves, which virtually travel several times through the experimental arrangement, are damped too strongly to have considerable influence on the resulting amplitude. A liquid with better properties than sodium can hardly be found, but an improvement may be obtained with an increase in linear dimensions. Experiments have been carried out with an ionized gas in a magnetic field.[14] At this stage, however, it may be premature to draw definite conclusions about the possibility of improving the conditions for magneto-hydrodynamic waves in the gas.

ACKNOWLEDGMENTS

I want to express my sincere thanks to Professor Hannes Alfvén for many valuable remarks on this work. I am also greatly indebted to Dr. N. Herlofson, Dr. S. Lundquist, and Mr. E. Åström for many stimulating discussions.

The investigation has been made possible by grants from Naturvetenskapliga Forskningsrådet.

[14] H. Bostick and M. A. Levine, Phys. Rev. **87**, 671 (1952).